

Intelligent maximum power point tracking control for solar photovoltaic systems using fuzzy and neuro-fuzzy techniques

Mohankumar Venugopal¹, Madhusudhan Mahadevaswamy², Manjunath Bimbitha Swarna Gowri³

¹Department of Artificial Intelligence and Machine Learning, Dr. Ambedkar Institute of Technology, Bangalore, India

²Department of Electrical and Electronics Engineering, Dr. Ambedkar Institute of Technology, Bangalore, India

³Department of Electronics and Communication Engineering, Atria Institute of Technology, Bangalore, India

Article Info

Article history:

Received May 22, 2025

Revised Sep 11, 2025

Accepted Sep 27, 2025

Keywords:

Fuzzy-logic controller
Maximum power point tracking
Neuro-fuzzy-controller
Power
Solar photovoltaic array

ABSTRACT

A solar-photovoltaic (PV) system cannot optimize power transfer from the generator to the load due to the nonlinear characteristics of the PV arrays. Maximum power point tracking (MPPT) approaches are necessary to optimize the power output of PV arrays. This study introduces a dual intelligent MPPT framework using fuzzy-logic controller (FLC) and neuro-fuzzy controller (NFC) to enhance solar PV efficiency under dynamic environmental conditions. The FLC uses 49 fuzzy rules with seven membership functions (MFs) in a fuzzy interface system (FIS). The NFC is an extension of FLC and is constructed using the artificial neuro-fuzzy interface system (ANFIS). The work analyzes the simulation results and performance realization, including % power loss, system efficiency, and MPPT efficiency under variable irradiance and temperatures. The solar-PV system utilizes FLC and NFC to achieve MPPT efficiencies of 97.89% and 98.61%, respectively. Similarly, the solar-PV system employing FLC and NFC yields system efficiencies of 98.24% and 99.23% respectively. The proposed system using both FLC and NFC is compared with existing MPPT approaches, with better improvement in system efficiency.

This is an open access article under the [CC BY-SA](#) license.



Corresponding Author:

Mohankumar Venugopal

Department of Electronics and Communication Engineering, Dr. Ambedkar Institute of Technology
Near Gnana Bharathi, 2nd Stage, Naagarabhaavi, Bengaluru, Karnataka, 560056, India

Email: phd.mohankumar@gmail.com

1. INTRODUCTION

The renewable energy sources significantly influence the production of electricity. The four types of renewable energy are hydro, geothermal, wind, and solar. The first human era made several uses of them for various purposes. These sources lessen the generation of greenhouse gases, such as carbon dioxide and nitrogen oxides, which cause climate change. Cutting-edge technologies are using these energies to generate incredible profits [1]. One rapidly developing technology is solar energy, which has affordable equipment costs. One of the most successful innovations is photovoltaic (PV) technology, which uses a PV cell, panel, or array to convert solar radiation into electric energy [2] directly. The photovoltaic effect is the PV system's direct light conversion into energy. PV power systems are classified according to their operational requirements, how their machinery is connected to other power sources, the arrangement of their components, electrical loads, and their efficiency. PV systems can be divided into two main categories: standalone and grid-connected [3]. The standalone system's construction aims to supply specific direct current (DC) and alternating current (AC) electric loads and an independent electric grid utility. Grid-connected PV systems use solar PV systems to generate power and are linked to the grid utilities. Solar PV arrays, power conditioning devices, converters, and grid-connected equipment are all part of the grid-connected system [4].

Since PV arrays are not linear, there is no maximizing of power transmission from PV generation to load usage in solar-based PV systems. These properties are determined mainly by external factors such as temperature and irradiance, which depend on the solar-PV cell's temperature and irradiance. PV efficiency is impacted by the power transfer from electricity to solar, making maximizing solar energy challenging [5]. Nonetheless, to continue supplying energy without experiencing a decline in performance, it is crucial to generate the PV system's maximum efficiency. The PV array's maximum power point (MPP) must be obtained to increase the PV system's power production. As a result, to maximize power from PV arrays and make efficient use of their power, maximum power point tracking (MPPT) techniques are required. The majority of current research offers a wide variety of MPPT-based techniques. Several factors, including cost, difficulty level, hardware needs, method of execution, converging speed, and many more, are considered while developing and implementing these MPPT techniques [6]. There are two types of MPPT approaches: soft computing and traditional. Incremental conductance (INC) and perturb and observe (PO) procedures are examples of conventional MPPT techniques. These conventional methods have moderate MPP tracking, a straightforward structure, and simple implementation. Changes in the MPP limit conventional techniques, causing a rapid impact on accuracy and a loss of usable power [7].

Intelligent and bio-inspired techniques are used to construct the soft-computing MPPT approaches. Examples of intelligent techniques are the genetic algorithm (GA), artificial neural networks (ANNs), and fuzzy-logic controllers (FLCs) [8]. When handling the nonlinear features of current (I)-voltage (V) and power (P)-voltage (V) curves, intelligent approaches need more processing but track the MPP more accurately and with a minor power loss. Bio-inspired MPPT techniques include cuckoo search (CS) engines, colony optimization, and particle swarm optimization (PSO) [9]. The bio-inspired MPPT algorithms offer superior exploration capabilities with minimal computational effort. Because the methods may quickly attain a global highest, they can minimize power loss regardless of settings with partial shading. The more gradual convergence of the bio-inspired MPPT techniques is a disadvantage that keeps them from being used as cloud-based alternatives in practical scenarios [10]. Table 1 illustrates the comparison of MPPT approaches.

Table 1. Comparison of MPPT approaches

MPPT techniques	Description	Strengths	Limitations
P&O [6]	Simple hill-climbing to track MPP	Low cost; easy to implement; requires minimal hardware	Steady-state oscillations; poor PS performance; drift under rapid changes
INC [7]	Uses the dI/dV relation for precise MPP detection	Better accuracy than P&O; reduced oscillation	Sensitive to noise; higher complexity
FLC [8]	Rule-based decision making for MPPT	Handles nonlinearities well; robust response	Rule design and tuning complexity
ANN [8]	Learns a nonlinear mapping between inputs and MPP	High accuracy; fast after training; adaptive	Requires a large dataset; offline training; risk of overfitting
GA [8]	Evolutionary optimization applied to MPPT	Global search: effective under complex conditions	Slower convergence; computationally intensive
PSO [9]	Swarm-based global optimization of MPP	Good accuracy under PS; global optimum search	Iterative and slower than conventional methods
Ant colony optimization (ACO) [9]	Mimics ant foraging to find the global MPP	Avoids local minima; strong exploration capability	Iterative process; parameter sensitivity
CS [9]	Uses Lévy flights for global MPP search	Robust exploration; fewer parameters than GA/PSO	Convergence speed variable; tuning needed

Problem statement: due to its widespread adoption in the last ten years, solar energy has seen an exponential surge in demand. Through the clean reception of light, energy, solar panels generate electricity. Solar panels are highly dependent on external factors such as temperatures and irradiance to produce the MPP. Due to the nonlinear IV properties of PV cells, the PV current also influences the PV's output voltage, which prevents the load impedance from directly forecasting the output power. Thus, a PV MPPT control system is required to reach the MPP of the PV. To ascertain the practical MPP, an observation control system continuously adjusts its operating position and changes the voltage or current state of the power input. Numerous methods for tracking the MPP have been published in the scientific literature. Nevertheless, most existing methods need improved accuracy, efficiency, and response time. Traditional MPPT methods struggle with accuracy and adaptability under fluctuating irradiance. This study proposes intelligent controllers to address these limitations intelligent controllers to address these limitations and this research aims to identify the most precise and adaptable mechanism for obtaining the required PV power under various environmental circumstances.

The work aims to develop an effective solar PV system and optimize its MPPT algorithm to maximize system efficiency under various environmental conditions. The work aims to develop intelligent controller-based MPPT algorithms for solar PV systems, such as FLC and neuro-fuzzy controller (NFC), which increase system efficiency by lowering power loss. In order to improve flexibility under changing temperature and irradiance conditions, an artificial neuro-fuzzy interface system (ANFIS)-based NFC is created, along with a 49-rule FLC with seven membership functions (MFs). The suggested solution outperforms traditional MPPT techniques in terms of both MPPT efficiency and system efficiency. Additionally, the NFC shows a great deal of promise in lowering power losses and enhancing PV systems' overall performance.

This section includes the work done on various MPPT techniques for PV systems to achieve performance parameters and system efficiency. Riquelme-Dominguez and Martinez [11] present PV-based MPPT methods employing a state-space framework in several test circumstances. This work studies the PO and drift-free-based MPPT approaches. At the EN50530 irradiance examination, the system achieves a dynamic efficiency of 96.77% and 96.77% for conventional PO and drift-free PO-based MPPT methods, respectively. Alcaide *et al.* [12] discuss the effect of MPPT techniques on capacitor longevity throughout the PV array. The work analyses the PV voltage and power outcomes using a PO-based MPPT technique. The PO and INC-based MPPT techniques provide 91.56% and 91.82% efficiency, respectively, for the system. Zouga *et al.* [13] present the backstepping control-based PSO for PV-based electrical networks under fluctuating loads. Backstepping and PSO processes design the PV voltage and power factor regulators. The study examined the injected current, DC-link, and PV voltage at different loads, both with and without control. Malarvili and Vinothkumar [14] present the artificial intelligence-based PSO for MPPT of solar energy systems under PSCs. The FLC—merged with PSO—is regarded as an artificial intelligence technique to enhance PV system efficiency under PSCs. With PSO and FLC+PSO under PSCs, the PV system achieves steady state convergence of 0.6 and 0.3 sec. Jamaludin *et al.* [15] describe the Salp-swarm algorithm (SSA)- based MPPT for PV systems under partial shade conditions (PSCs). When operating under uniform illumination conditions (UICs), the system achieves 97.87% tracking efficiency using the SSA. Bouakkaz *et al.* [16] present the FL-based modified Hill climbing (MHC) MPPT technique with adaptive step characteristics for PV systems. To build the MHC, the FLC output response is attached to the HC method. This paper analyses the PV and boost-converter findings.

Hayder *et al.* [17] discuss FLC-based MPPT for PV systems. This work investigates the changing irradiance and temperature conditions of solar PV and IV and includes the duty cycle, voltage, current, and power results under various temperature and irradiance circumstances. Salem *et al.* [18] describe the PO and FLC-Hill climbing (HC)-based MPPT techniques for PV generators. The study covers the individual algorithms for PO, FLC, and FLC-HC. They discuss the PV system outcomes utilizing FLC-HC and PO. Ali *et al.* [19] present the FLC-INC-based MPPT technique with variable-step capabilities for grid-connected solar energy systems. The grid-connected PV system analyses solar PV and IV. The duty cycle, voltage, current, and power outcomes under various temperature and irradiance circumstances are included in the work. Bag *et al.* [20] cover the combined sliding-mode control (SMC) and reinforcement learning (RL)—based MPPT technique for grid-connected PV systems. The hybrid model achieves a THD of 2.95% for load voltage in steady-state settings and provides 98.80% efficiency. Roy *et al.* [21] address the comparative study of ANN based MPPT energy harvesting techniques for solar-PV systems. Using ANN-based methods, the maximum PV voltage at various temperatures and irradiances is analyzed. Padmanaban *et al.* [22] describe the ANN and Newton-Raphson (ANN-NR) based selective harmonic elimination (SHE) strategy in the cascaded multilevel inverter (CMLI) for PV applications. By employing a symmetric technique, the PV system achieves an efficiency of 89.39% with a power loss of 97.73 W. Similarly, by employing the symmetrical technique with ANN-NR, the PV system achieves an efficiency of 93.14% with a power loss of 58.64 W. Table 2 shows the summary of existing works using various approaches on the solar-PV system.

The efficiency and dynamic response of current MPPT techniques are increased, but accuracy, convergence speed, computational complexity, and real-time application are all traded off. Under partial shading, conventional methods perform poorly, whereas intelligent and hybrid methods become more difficult and expensive. Efficiency and power quality are rarely optimized together in studies. Therefore, this study aims to address the market gaps for an MPPT method that ensures high efficiency, rapid tracking, and adaptability with reduced implementation complexity.

Table 2. Summary of existing works

Authors (Ref.)	Method	Results	Advantages	Limitations
Riquelme-Dominguez and Martinez [11]	PO and drift-free PO (state-space)	Dynamic efficiency: 96.77% (both PO and drift-free PO) at EN50530 test	High dynamic efficiency; drift-free reduces oscillations	Limited to test conditions; scalability to large PV arrays not shown
Alcaide <i>et al.</i> [12]	PO and INC	PO: 91.56% efficiency, INC: 91.82% efficiency	Good efficiency under the capacitor longevity study	Lower efficiency compared to advanced techniques; limited dynamic testing
Zouga <i>et al.</i> [13]	Backstepping + PSO	Improved current injection, DC-link, and PV voltage under varying loads	Handles load fluctuation; better power factor regulation	Computationally complex; requires tuning of backstepping+PSO
Malarvili and Vinothkumar [14]	FLC + PSO (AI-based)	Steady-state convergence: 0.6 sec (PSO), 0.3 sec (FLC+PSO) under PSCs	Fast convergence under PSCs; hybrid improves efficiency	Requires fuzzy rule base; sensitive to parameter tuning
Jamaludin <i>et al.</i> [15]	SSA	97.87% tracking efficiency under UICs	High efficiency; effective under PSC and UICs	Performance under highly dynamic PSCs is not fully addressed
Bouakkaz <i>et al.</i> [16]	FLC-based MHC	Improved PV and boost converter (BC) performance	Adaptive step size improves tracking; avoids oscillations	Complexity increases; it depends on the fuzzy system's accuracy
Hayder <i>et al.</i> [17]	FLC-based MPPT	Duty cycle, voltage, current, and power were analyzed under varying irradiance.	Handles irradiance/temperature variations	Performance metrics (efficiency %) not quantified
Salem <i>et al.</i> [18]	PO, FLC, and FLC-HC	PV system tested with individual PO and hybrid FLC-HC	Hybrid FLC-HC outperforms conventional PO	Implementation complexity; lacks quantitative efficiency data
Ali <i>et al.</i> [19]	FLC-INC (variable step)	Grid-connected PV analyzed under varying conditions	Variable-step improves adaptability; grid-connected application	Increased computational demand; system complexity
Bag <i>et al.</i> [20]	Sliding mode control + RL	Achieves 98.80% efficiency; THD=2.95% in steady state	High efficiency; low THD; adaptive learning capability	Computationally intensive; may require large training datasets
Roy <i>et al.</i> [21]	ANN-based MPPT	PV voltage at various temperatures and irradiances analyzed	Learns nonlinear PV characteristics; adaptable	Requires training; performance depends on dataset quality
Padmanaban <i>et al.</i> [22]	ANN-NR, SHE	Efficiency: 89.39% (ANN), 93.14% (ANN-NR); Loss: 97.73 W vs 58.64 W	Reduced power loss with ANN-NR; improved SHE	Lower efficiency compared to other AI techniques; implementation complexity

2. PROPOSED WORK

The two MPPT algorithms, including FLC and NFC, are implemented in this study. The difficulty, expense, speed of convergence, and ease of implementation of these algorithms may all differ. The work involves implementing various MPPT techniques in varying temperature and irradiance circumstances to determine the power supplied by the solar-PV array. The solar-PV array's MPPT technique will increase the dependability and efficiency of MPP. Implementing the MPPT algorithms, which adapt dynamically for extracting the MPP in the solar-PV system, is essential. The main parts of the design model are a 250 W solar PV array panel, a DC-DC-based pulse width modulation (PWM) generator, an MPPT controller with FLC/NFC techniques, and a BC with the necessary load. The MPPT mechanism based on solar PV is shown in Figure 1. The BC gives the solar PV-based MPPT system's output voltage, current, and power values. After receiving the temperature and irradiance data, the PV array model delivers the PV voltage, current, and power in DC. The DC-to-DC-based BC receives the PV-based DC voltages, which use an MPPT controller to transform them to DC. Two MPPT techniques, including NFC and FLC, are used in constructing the MPPT controller. The duty cycle (D) is supplied by the MPPT controller and sent into the PWM generator. At the switching frequency of 10 kHz, the PWM generator gets the duty cycle and produces the gate pulses. The insulated-gate bipolar transistor (IGBT) of the BC makes additional use of these gate pulses. A load resistor is attached to this BC to calculate the resulting power of the solar PV-based MPPT system.

The solar PV module produces the PV and VI graphs under different operating circumstances, such as temperature and irradiance. Determining the MPP from the PV curve is challenging. Therefore, the DC-DC-based BC with an MPPT control mechanism is required to overcome these problems. Several algorithms are used to determine the MPPT control mechanism. The solar-PV module and the load resistance are interfaced through this DC-DC converter. The BC reaches the designated DC output voltage by increasing the obtained input PV voltage. In Figure 2, the BC representation is depicted. CR (capacitor (C_{out}) and load resistor (R_L) in parallel, input capacitance (C_{in})), an IGBT-followed diode as the inductance, and a gate pulse from a PWM generator are the critical components of the BC. Inductance (L) is connected to the BC, which collects the input voltage from the PV array. The parallel C_{in} and L of the IGBT module serve as a switch and link it to the BC input. Situated in parallel to CR, the diode functions as an additional switch.

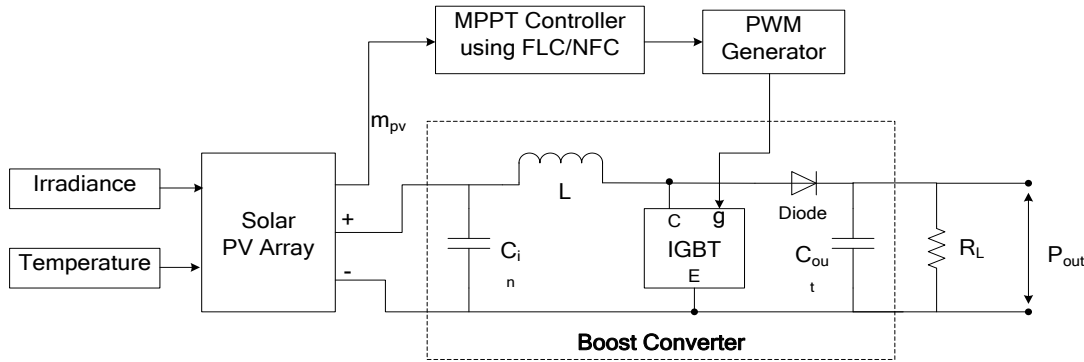


Figure 1. Solar-PV system using MPPT controller

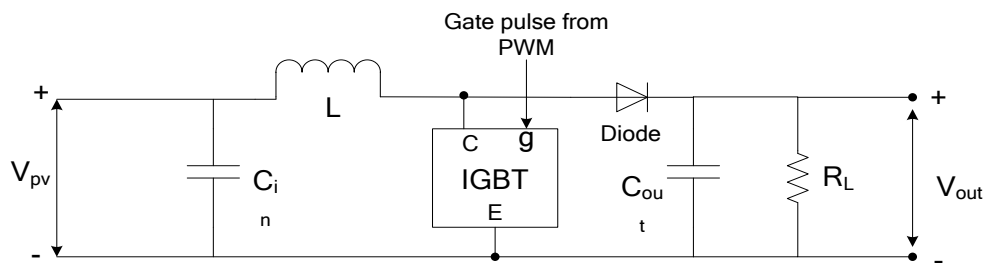


Figure 2. DC-DC-based BC

The load resistor is connected across the voltage sensor unit to produce the anticipated final DC output voltage (V_{out}). A steady input current is produced using an inductance link to the PV voltage. The MPPT controller uses PWM to operate the IGBT switch in both "ON" and "OFF" modes. The DC to DC-based PWM generators' gate pulses are linked to the IGBT switch end. The PWM generator produces gate pulses with a switching frequency of 10 kHz. With the diode "ON" and the switch "OFF," the polarity of the inductor is changed. To maintain the current's flow direction, the inductor releases the accumulated energy and transfers it to the resistor. The final power (P_{out}) is computed using the final voltage (V_{out}) and current (I_{out}). The output of the BC is the DC output voltage and current. In (1) can be used to express the DC output current of the BC as (1):

$$I_{out}(a) = \frac{(1-D)V_{out}(a-2)I_{pv}(a-1)}{2V_{out}(a-2)-V_{out}(a-3)} \quad (1)$$

2.1. Fuzzy-logic controller

For industry sectors, the FLC is more efficient than the conventional PID controller and provides more options for output response. Failsafe execution, fast information set interpretation, and fault tolerance are only a few of the FLC's benefits. The five main components of the FLC operation are the evaluation unit, ruleset, fuzzification, defuzzification, database, and MPPT (which functions as the plant). The FLC operating with the MPPT is seen in Figure 3. The fuzzification process changes the absolute (crisp) value into a fuzzy (linguistic) value. PV values (power and voltage) give the input data (error signal) for the fuzzification process, as crisp data into variables (fuzzy variables). The fuzzy variables can detect fuzzy values and act as fuzzy sets. The MFs deal with the fuzzy sets in the small, high, low, or massive values.

The rule base, which consists of fuzzy rules based on the MFs, improves the efficiency of the plant. The assessment process provides the decision logic predicated on the rules stored in the database. The essential logic operations AND, OR, and NOT implement the fuzzy rules. As the defuzzification process progresses, the fuzzy values become crisp values. Three key components are utilized in FLC activities: MFs, fuzzy rules, and fuzzy variables.

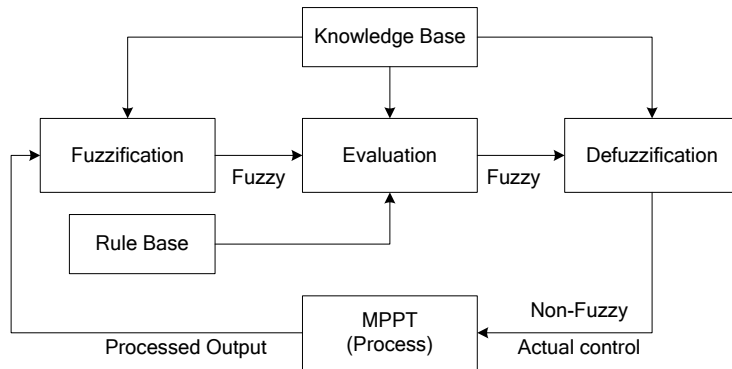


Figure 3. FLC with MPPT

Fuzzy variables: considering the Mamdani model, the FLC is designed using the fuzzy interface system (FIS) in the MATLAB Simulink environment. The FLC variables error (E) value and change in error (CE value) are defined as follows using (2) and (3). PV power is measured using $P(a)$ and $P(a-1)$. PV voltages $V(a)$ and $V(a-1)$ represent the current and previous values. The prior error input value is $E(a-1)$. Figure 4 depicts the formation of errors and CE indications for FLC. PV power and voltage values are inputted into (2) to determine the error (E) estimate.

$$E(a) = \frac{P(a) - P(a-1)}{V(a) - V(a-1)} \quad (2)$$

$$CE(a) = E(a) - E(a-1) \quad (3)$$

Membership function: using fuzzy set MF, the fuzzy components E, CE, and FLC output (FO) values for the given discourse domain are shown in the interval [-500 to 500]. The range of possibilities for MFs for E and CE is based on the triangular-shaped MFs. The range decision of the FLC output (FO) MF is based on the triangle-shaped MF. Indicators for performance and robustness will rise with a triangle-shaped MF inside certain bounds. Positive large (PB), positive medium (PM), positive small (PS), zero (ZO), negative big (NB), negative medium (NM), and negative small (NS) are the seven fuzzy variables (FVs) and act as MFs that the E and CE use. The fuzzy variables are retained in the knowledge base and will be used later in the rule-building process. MFs are categorized as tiny or large based on their range.

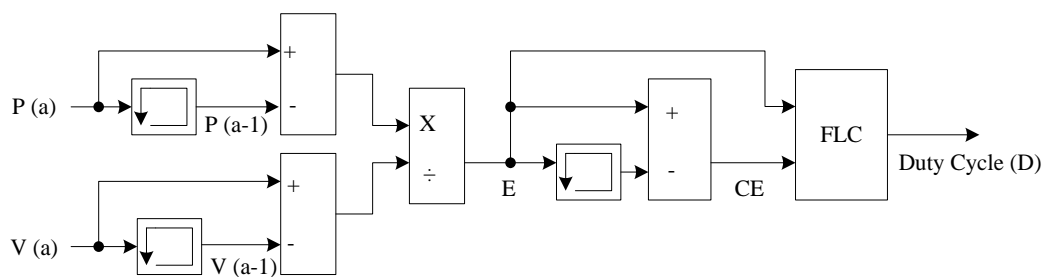


Figure 4. Error and CE generation used in FLC

Fuzzy rules: about the rule set, the rule base is created using the fuzzy rules. The collection of fuzzy rules is shown in Table 3. The Mamdani-based FIS is used in the construction of the FLC system. Forty-nine rules and 7 MFs are used in FIS for the E and CE variables. This rule set contains 49 fuzzy rules that can generate a single FO output as Duty cycle (D) for two inputs. The FLC output is produced based on (4) as follows for the n^{th} -order rule base. For the n^{th} fuzzy rule set, $n=1, 2, \dots, N_m$. The integer (i) is set to 1, 2, 3, 4, 5, 6, and 7. Employing the centroid technique, the ruleset is transformed into a clean output structure to complete defuzzification.

Rn: IF (error is E (i)) AND (Change in Error is CE (i)) then (FLC output is FO (i)) (4)

Table 3. FLC rule set used for MPPT process

Error/CE	NB	NM	NS	ZO	PS	PM	PB
NB	NB	NB	NB	NM	NM	NS	ZO
NM	NB	NB	NB	NM	NS	ZO	PS
NS	NB	NM	NS	NS	ZO	PS	PM
ZO	NM	NM	NS	ZO	PS	PM	PM
PS	NM	NS	ZO	PS	PS	PM	PB
PM	NS	ZO	PS	PM	PM	PB	PB
PB	ZO	PS	PM	PM	PB	PB	PB

The controller can capture nonlinear variations in PV output without becoming overly complex due to the use of seven MFs for each input variable, which strikes a delicate balance between resolution and computational efficiency. This setup yields $7 \times 7 = 49$ fuzzy rules with two inputs (E and CE), which is enough to cover every circumstance in which the PV system could operate. This rule-based approach improves robustness under dynamic irradiance and partial shading, minimizes steady-state oscillations, and guarantees seamless transitions between control actions. It is the best option for real-world MPPT applications since keeping the rule set at 49 preserves real-time implementation feasibility on digital controllers.

2.2. Neuro-fuzzy-controller

The NFC extends FLC using an ANFIS. The FIS of NFC is automatically realized by neural networks (NNs). The practical process of converting from crisp to fuzzy and vice versa is provided by NFC. The ANFIS framework is used to construct the FIS optimization using NNs. Figure 5 illustrates the implementation of NFC operation through ANFIS. Training and testing the FIS is possible, and the NFC has the unique ability to learn fresh abilities. The four primary operations are FIS generation, training data unit, FIS testing, and FIS training.

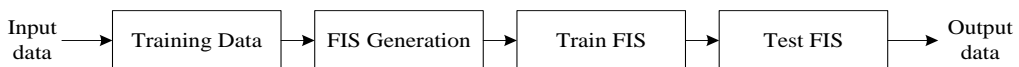


Figure 5. ANFIS-based NFC implementation

For NFC training, the PV power and voltage data are considered. The ANFIS editor for NN training loads these data. Grid partitioning is the method used to generate FIS. The FIS produces the constant MF output after considering the seven MFs with a kind of Gaussian MF as input. The FIS employs seven rules and the AND operation to produce a single FIS output. Two optimization strategies—back-propagation and hybrid mode—can be used for FIS training. This work considers the hybrid optimization strategy to train the FIS. With three epochs, the error tolerance is set to zero. To produce the final NFC output, test the FIS against the training data when it has finished training. The final NFC output is the FIS output generated during the testing process. The NFC output is utilized in PWM generators and is regarded as a duty cycle.

Hybrid optimization was chosen because it combined the benefits of back-propagation and least-squares estimation. Slow and prone to local minima is simple back-propagation. Least-squares evaluation is fast for linear parameters but poor for nonlinear ones. Both are balanced in the hybrid technique, which ensures faster convergence and higher precision. ANFIS significantly reduces training timeframes by avoiding local minima and achieving robust adjustment of MFs and rule parameters. This makes it ideal for MPPT, where speed and accuracy are critical.

3. RESULTS AND DISCUSSION

This section discusses the outcomes of the solar PV-based system using intelligent MPPT control approaches. The comprehensive simulation results, including the ultimate output (voltage (V), current (I), and power (P)) utilizing FLC and NFC, are described at various temperatures and irradiances. Performance metrics like power loss, PMPPT efficiency and system efficiency are realized under various conditions. The solar-PV array and cell specifications and values considered for the suggested design model are listed in Table 4. The proposed Simulink model for intelligent MPPT control in solar PV systems is illustrated in Figure 6.

Table 4. Specification of the solar PV-based system with MPPT controllers

Parameters	Specific values and units
Parallel strings and series-connected modules/string	1, 1
Irradiance (W/m^2)	[200 400 600 800 1000]
Temperature ($^{\circ}\text{C}$)	[0 25 50 75 100]
Open circuit voltage (V_{oc}), short circuit current (I_{sc})	50.93 V, 6.2 A
Voltage and current at MPP ($V_{\text{mp}}, I_{\text{mp}}$)	42.8 V, 5.84 A
Number of cells per module (N_c)	72
Diode ideality factor (D_{if}) and saturation current (I_{ds})	1.0263, $1.3617 \times 10^{-11} \text{ A}$
Series and shunt resistance (R and R_s)	$0.377759 \Omega, 448.69 \Omega$
Simulation time (Sec)	[0, 0.5, 1, 1.5, 2]

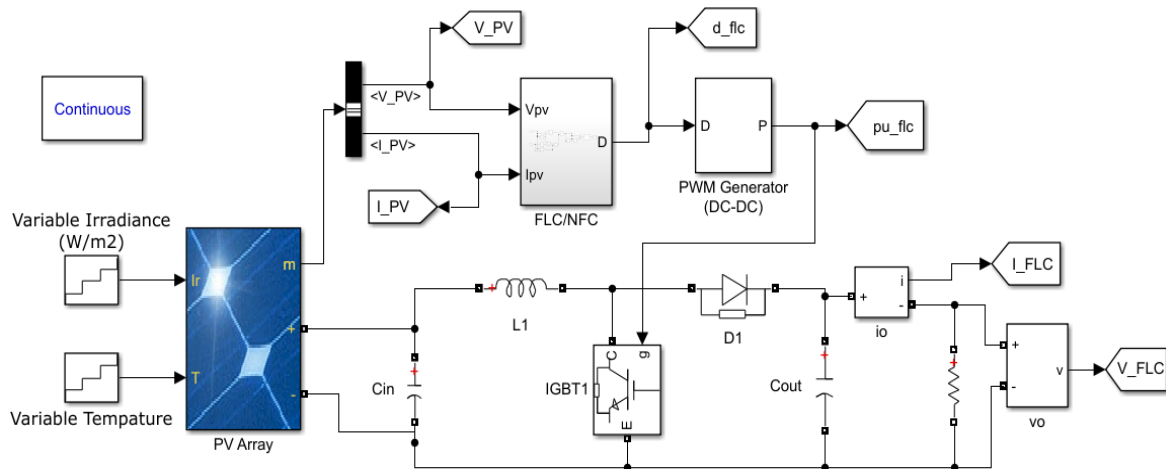


Figure 6. Proposed Simulink model for intelligent MPPT control in solar PV systems

Figure 7 shows the simulation results of a solar-PV system using MPPT controllers under varying irradiance at 25°C . Figures 7(a) and (b) show the BC output findings (V , I , and P) for FLC and NFC, respectively. By employing FLC, the BC output power is raised from 12.23 W to 244.7 W at 25°C , with an irradiation of 200–1000 W/m^2 . Furthermore, at 25°C and an irradiation of 200–1000 W/m^2 , the BC output power utilizing NFC is enhanced from 12.23 W to 246.5 W.

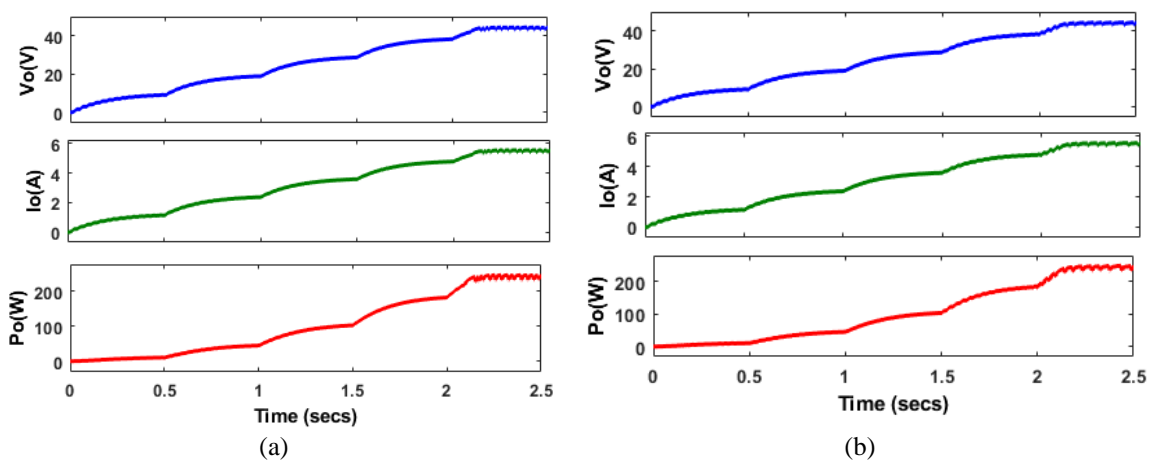
Figure 7. Simulation results at variable irradiance at 25°C for; (a) FLC and (b) NFC

Figure 8 shows the MPPT controller outcomes employing FLC and NFC. Figures 8(a) and (b) display the FLC and NFC outputs at 1000 W/m^2 and 25°C , respectively. Both the controller outputs vary from -10 to 10. The FLC output is generated based on the fuzzy rule sets and the NFC output is generated using PV values based on the FIS training.

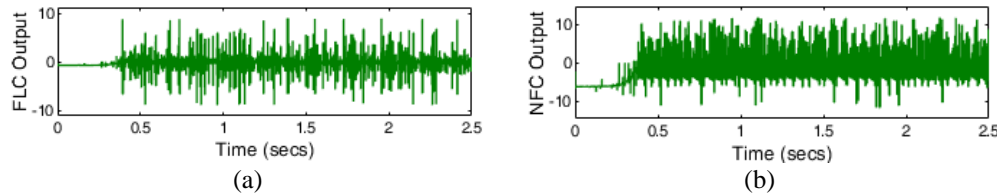


Figure 8. MPPT controller outputs at variable irradiance at 25 °C for; (a) FLC (b) NFC

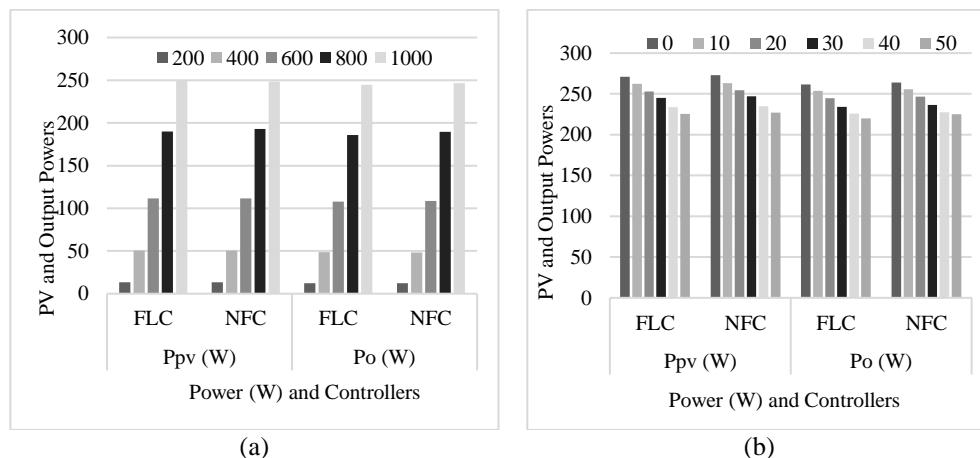
The performance summary of the solar-PV system using FLC and NFC at 1000 W/m² and 25 °C is tabulated in Table 5. The percentage of power loss is calculated based on the difference between the PV and output power and multiplied by 100. The MPPT efficiency is the ratio of the obtained PV power to the actual PV power. The system efficiency is the ratio of the obtained output power by PV power. The PV-power (Ppv) and output power (Po) of the solar-PV system using FLC are 249.1 W and 244.7 W, respectively.

Similarly, the solar-PV system using NFC obtains the PV power (Ppv) and output power (Po) of 248.4 W and 246.5 W, respectively. The FLC-based approach offers better PV power; however, NFC offers better-obtained power than FLC, which boosts the system and MPPT efficiency. The solar-PV system obtains the power loss of 4.4% and 1.9% using FLC and NFC, respectively. The solar-PV system obtains the MPPT efficiency of 97.89% and 98.61% using FLC and NFC, respectively. Similarly, the system efficiency of 98.24% and 99.23% is obtained for solar-PV systems using FLC and NFC, respectively. The power loss is reduced by around 56% using NFC than FLC in the solar-PV system. The MPPT and system efficiency are improved by around 0.74% and 0.99% using NFC than FLC in the solar-PV system.

The PV and output power results using MPPT algorithms are illustrated in Figure 9. The PV and output powers using FLC and NFC at Variable irradiance (200 to 1000 W/m²) at 25 °C are shown in Figure 9(a). The PV and output powers using FLC and NFC at different temperatures (0 to 50 °C) at 1000 W/m² irradiance are shown in Figure 9(b). The PV output power using FLC declined from 271.1 W to 225.3 W and 272.8 W to 227.01 W using NFC at 1000 W/m², with different temperatures (0 to 50 °C). By employing FLC, the BC output power declined from 261.62 W to 220 W at 1000 W/m², with different temperatures (0 to 50 °C).

Table 5. Performance summary of solar-PV system using FLC and NFC at 1000 W/m² and 25 °C

Parameters	FLC	NFC
Vpv (V)	42.05	41.72
Ipv (A)	5.925	5.955
Ppv (W)	249.1	248.4
Vo (V)	44.25	44.41
Io (A)	5.531	5.551
Po (W)	244.7	246.5
Power loss (W) (%)	4.4	1.9
MPPT efficiency (%)	97.89	98.61
System efficiency (%)	98.24	99.23

Figure 9. PV and output power results using various MPPT algorithms at; (a) variable irradiance at 25 °C and (b) different temperatures at 1000 W/m²

Furthermore, the BC output power utilizing NFC is decreased from 263.8 W to 224.9 W. As the irradiance value rises at 25 °C, the PV and output power values also rise. At 1000 W/m², the PV and output power values decline when the temperature rises. Compared to the FLC technique, the solar PV system with NFC yields better PV and output power (average) outcomes.

The % power loss (W) using MPPT algorithms is illustrated in Figure 10. The % power loss (W) using FLC and NFC under variable irradiance (200 to 1000 W/m²) at 25 °C is shown in Figure 10(a). The NFC-based solar-PV system reduces the power loss by 16.6%, 23.25%, and 56.8% at 600, 800, and 1000 W/m² than the FLC-based approach. However, there is no power loss at 200 and 400 W/m² using FLC and NFC. The % power loss (W) using FLC and NFC at different temperatures (0 to 50 °C) under 1000 W/m² irradiance is shown in Figure 10(b). The NFC-based solar-PV system reduces the significant power losses at 0, 10, 20, 30, 40, and 50 °C temperatures under 1000 W/m² than the FLC-based approach.

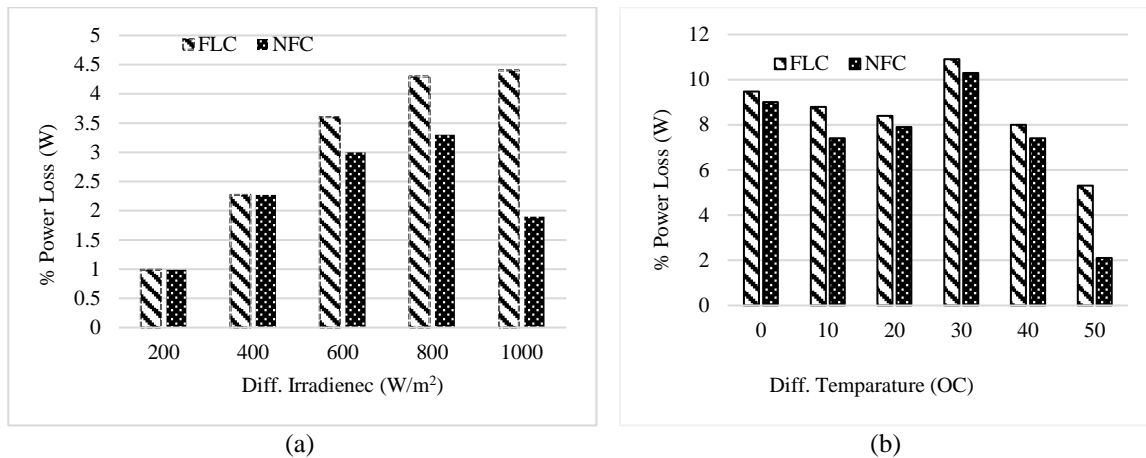


Figure 10. % power loss (W) using various MPPT algorithms at; (a) variable irradiance at 25 °C and (b) diff. temperatures at 1000 W/m²

The system efficiency (%) using MPPT algorithms is illustrated in Figure 11. The system efficiency (%) using FLC and NFC under variable irradiance (200 to 1000 W/m²) at 25 °C is shown in Figure 11(a). The NFC-based solar-PV system improves the system efficiency by 0.54% and 0.76% at 800 and 1000 W/m² than the FLC-based approach. However, system efficiency remains the same at 200 and 600 W/m² using both FLC and NFC. The system efficiency (%) using FLC and NFC at different temperatures (0 to 50 °C) under 1000 W/m² irradiance is shown in Figure 11(b). The NFC-based solar-PV system improves system efficiency at 0, 25, 50, 75, and 100 °C temperatures under 1000 W/m² than the FLC-based approach.

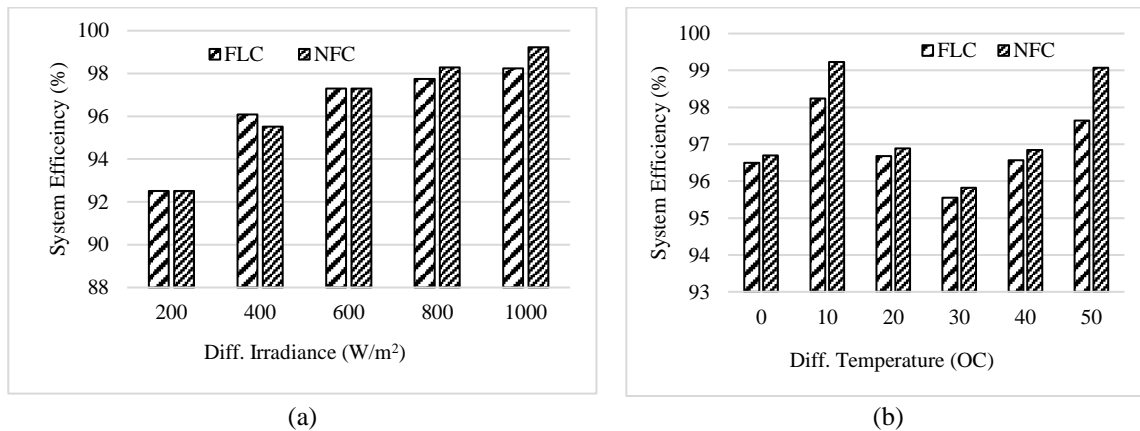


Figure 11. System efficiency (%) concerning the various MPPT algorithms at; (a) variable irradiance at 25 °C and (b) diff. temperatures at 1000 W/m²

The performance comparison of proposed MPPT approaches with existing MPPT approaches [23]-[31] is illustrated in Table 6. The comparative realization includes the MPPT approach used, constant or variable irradiance, rated power (W), obtained PV power, output power and system efficiency (%) in this work. The proposed FLC-based MPPT approach offers better system efficiency than adaptive PO [23] by 3.65%, improved PO [24] by 3.02%, INC+PSO approach [25] by 1.27%, PO+PSO-based approach [26] by 6%, FLC [27] by 3.19%, and FLC [28] by 2.28% under constant and variable irradiance conditions. Similarly, the proposed NFC-based MPPT approach offers better system efficiency than NFC [29] by 0.2%, artificial bee colony (ABC) with NFC [30] by 0.9% and the NFC approach by 0.7% under variable irradiance conditions. Overall, the proposed solar-PV system with FLC and NFC approach offers better system efficiency than other MPPT controller approaches.

Future research should address dynamic load changes and battery non-linearities, as the current study assumes optimal battery performance and a stable load, which may not accurately represent real-world PV systems. Comparisons of FLC, NFC, and conventional approaches' performance should also be subjected to statistical significance testing. This will verify if the efficiency gains (97.89–99.23%) that have been noted are statistically significant and not the result of chance fluctuations.

Table 6. Performance comparison of proposed MPPT approaches with existing MPPT approaches

Designs	MPPT approach	Irradiance (W/m ²)	Rated -PV power	PV power (W)	Output power (W)	Efficiency (%)
Ref. [23]	Adaptive PO	Constant	3000 W	2787	2637	94.65
Ref. [24]	Improved PO	Constant	250 W	240.8	229.41	95.27
Ref. [25]	INC+PSO	Variable	800	723.7	702	97
Ref. [26]	PO+PSO	Variable	250	243.69	225.03	92.34
Ref. [27]	PID	Variable	500	476.25	437.29	91.82
Ref. [27]	FLC	Variable	500	495.7	471.5	95.1
Ref. [28]	FLC	Constant	181	180.1	172.9	96
Proposed work	FLC	Variable	250	249.1	244.7	98.24
Ref. [29]	NFC	Variable	60	54.54	54.01	99.06
Ref. [30]	ABC+NFC	Variable	230	224.4	228.07	98.39
Ref. [31]	NFC	Variable	440	426	420	98.59
Proposed work	NFC	Variable	250	248.4	246.5	99.23

3.1. Discussion

This study optimizes MPPT performance by modelling an effective solar-PV system using intelligent controllers, namely the FLC and the NFC. According to the simulation findings, which were performed in MATLAB Simulink with varying irradiance, the NFC-based method considerably lowers power loss (1.9%) in comparison to the FLC-based system (4.4%). With an MPPT tracking improvement of 0.74% and an overall system efficiency improvement of 0.99% over the FLC-based technique, the NFC method achieves 98.61% MPPT efficiency and 99.23% system efficiency. Furthermore, NFC uses less energy and has better tracking accuracy than FLC, reducing power loss by 56%.

Prior MPPT optimization research has mostly focused on traditional techniques like PO and INC, which have limitations in dynamic irradiance conditions. Rule-based approximations still restrict the efficiency of FLC-based MPPT systems, although they have shown themselves to be more adaptable than conventional methods. Recent studies have shown that MPPT control can be enhanced by neuro-fuzzy techniques that integrate adaptive learning capabilities. These claims are supported by the study's results, which further validate the value of AI-driven controllers in solar PV systems by demonstrating that the NFC-based MPPT system outperforms FLC in reducing power loss and improving energy extraction.

Although the NFC-based MPPT controller is more effective in terms of tracking accuracy and energy efficiency, further research is needed to assess its scalability and real-time deployment in large-scale solar farms. Future studies can include hardware-in-the-loop (HIL) testing to validate both transient and steady-state reactions in practical settings. Furthermore, employing RL-based MPPT approaches could further enhance power tracking by dynamically altering control settings in real time. Future studies could also look at how clever MPPT controllers affect hybrid energy storage systems to maximize power distribution between solar PV arrays and battery storage components [32]-[34].

In conclusion, the proposed solar-PV system that makes use of intelligent controllers significantly enhances MPPT performance and overall system efficiency. By using NFC-based control, the system offers more accuracy, less power loss, and improved adaptability as compared to FLC-based techniques. These findings show that solar energy harvesting can be maximized through the application of AI-driven MPPT

techniques. As solar PV technology advances and drives the transition to sustainable and efficient energy sources, intelligent control techniques will be crucial to optimize the use of renewable energy sources.

Scalability is a feature of the suggested NFC-based MPPT for grid-connected and multi-panel configurations. While appropriate coordination with DC-link and current control loops assures stability in grid-connected operation, it can be applied at the central level for cost efficiency or at the module level for greater partial shading tolerance. Due to its modest computational effort, the NFC can be implemented in real-time on DSPs, MCUs, or FPGAs. Practical deployment is supported by precise sensing, fixed-point arithmetic, and efficient PWM synchronization; nonetheless, to guarantee dependable operation, hardware limitations like ADC resolution, EMI resilience, and protection procedures must be addressed.

4. CONCLUSION

The efficient solar-PV system using intelligent controllers (FLC and NFC) is modelled in this article to enhance the system efficiency. The solar-PV system has solar-PV arrays, a DC-DC-based BC with an MPPT controller, and a pulse generator. The intelligent controllers are used to track the PV arrays' best possible MPP. The proposed system is modelled using the MATLAB Simulink tool. The simulation results and controller outcomes are analyzed under variable irradiance conditions.

An important development in solar energy systems is an intelligent controller-based MPPT technique. The NFC-based MPPT controller demonstrates superior adaptability and efficiency, making it suitable for real-time solar PV applications. Intelligent MPPT controllers will be essential for optimizing solar power use as the use of renewable energy sources increases. By employing intelligent controller-based MPPT techniques, the suggested system provides increased system efficiency with reduced power loss in a range of environmental circumstances.

More processing is required by intelligent controllers, and digital signal processors (DSPs) and contemporary embedded systems have grown incredibly powerful and economical. Furthermore, intelligent MPPTs increase precision, lower power losses, which eventually result in larger energy savings that exceed their initial hardware expense. Adaptive learning is a feature of intelligent MPPT controllers that allows them to dynamically adjust their parameters while in use. Enhancing efficiency, adaptability, and integration with the latest technologies will be the main goals of future studies in intelligent controller-based MPPT approaches. For renewable energy systems to be widely adopted, AI-driven self-study, fault-tolerant, and grid-interactive MPPT control systems will be essential. Studies can help optimize solar energy consumption, along with contributing to a greener and energy-efficient future by developing such technologies.

FUNDING INFORMATION

Authors state no funding involved.

AUTHOR CONTRIBUTIONS STATEMENT

This journal uses the Contributor Roles Taxonomy (CRediT) to recognize individual author contributions, reduce authorship disputes, and facilitate collaboration.

Name of Author	C	M	So	Va	Fo	I	R	D	O	E	Vi	Su	P	Fu
Mohankumar	✓	✓	✓	✓		✓	✓	✓	✓	✓	✓	✓	✓	✓
Venugopal														
Madhusudhan		✓		✓	✓	✓	✓		✓	✓	✓			✓
Mahadevaswamy														
Manjunath Bimbitha	✓			✓			✓	✓	✓	✓				✓
Swarna Gowri														

C : Conceptualization

M : Methodology

So : Software

Va : Validation

Fo : Formal analysis

I : Investigation

R : Resources

D : Data Curation

O : Writing - Original Draft

E : Writing - Review & Editing

Vi : Visualization

Su : Supervision

P : Project administration

Fu : Funding acquisition

CONFLICT OF INTEREST STATEMENT

Authors state no conflict of interest.

DATA AVAILABILITY

Data availability does not apply to this paper as no new data were created or analyzed in this study.

REFERENCES

- [1] R. Wengenmayr and T. Bührke, *Renewable Energy: sustainable energy concepts for the future*. John Wiley & Sons, 2008.
- [2] R. Sims, "Energy for tomorrow's world. A renewable energy perspective," *Renewable Energy World*, vol. 3, no. 4, pp. 24–30, 2000.
- [3] F. Mehmood, N. Ashraf, L. Alvarez, T. N. Malik, H. K. Qureshi, and T. Kamal, "Grid integrated photovoltaic system with fuzzy-based maximum power point tracking control along with harmonic elimination," *Telecommunications Technologies*, vol. 33, no. 2, p. e3856, 2022, doi: 10.1002/ett.3856.
- [4] C. Mehdipour and F. Mohammadi, "Design and analysis of a standalone photovoltaic system for footbridge lighting," *Journal of Solar Energy Research*, vol. 4, no. 2, pp. 85–91, 2019, doi: 10.22059/jser.2019.283926.1120.
- [5] S. Balakrishna, A. Nabil, G. Thansoe, A. S. Rajamohan, and C. J. Kenneth, "The study and evaluation of maximum power point tracking systems," in *International Conference on Energy and Environment*, 2006, pp. 17–22.
- [6] J. P. Ram, T. S. Babu, and N. Rajasekar, "A comprehensive review on solar PV maximum power point tracking techniques," *Renewable and Sustainable Energy Reviews*, vol. 67, pp. 826–847, 2017, doi: 10.1016/j.rser.2016.09.076.
- [7] N. Karami, N. Moubayed, and R. Outbib, "General review and classification of different MPPT Techniques," *Renewable and Sustainable Energy Reviews*, vol. 68, pp. 1–18, 2017, doi: 10.1016/j.rser.2016.09.132.
- [8] Z. M. S. Elbarbary and M. A. Alranini, "Review of maximum power point tracking algorithms of PV system," *Frontiers in Engineering and Built Environment*, vol. 1, no. 1, pp. 68–80, 2021, doi: 10.1108/febe-03-2021-0019.
- [9] B. Pakkiraiah and G. D. Sukumar, "Research survey on various MPPT performance issues to improve the solar PV system efficiency," *Journal of Solar Energy*, vol. 2016, pp. 1–20, 2016, doi: 10.1155/2016/8012432.
- [10] K.-H. Chao, L.-Y. Chang, and H.-C. Liu, "Maximum power point tracking method based on modified particle swarm optimization for photovoltaic systems," *International Journal of Photoenergy*, vol. 2013, pp. 1–6, 2013, doi: 10.1155/2013/583163.
- [11] J. M. Riquelme-Dominguez and S. Martinez, "Systematic Evaluation of Photovoltaic MPPT Algorithms Using State-Space Models Under Different Dynamic Test Procedures," *IEEE Access*, vol. 10, pp. 45772–45783, 2022, doi: 10.1109/ACCESS.2022.3170714.
- [12] M. Alcaide *et al.*, "The Influence of MPPT Algorithms in the Lifespan of the Capacitor Across the PV Array," *IEEE Access*, vol. 10, pp. 40945–40952, 2022, doi: 10.1109/ACCESS.2022.3164411.
- [13] S. Zouga, M. Benchagra, and A. Abdallah, "Backstepping Control Based on the PSO Algorithm for a Three-Phase PV System Connected to the Grid under Load Variation," *2020 International Conference on Electrical and Information Technologies (ICEIT)*, Rabat, Morocco, 2020, pp. 1–6, doi: 10.1109/ICEIT48248.2020.9113235.
- [14] S. Malarvili and S. Mageshwari, "Artificial Intelligent Parameter based PSO for Maximum Power Point Tracking of PV Systems under PSC," in *2021 IEEE 17th International Colloquium on Signal Processing & Its Applications (CSPA)*, Langkawi, Malaysia, 2021, pp. 86–91, doi: 10.1109/CSPA52141.2021.9377286.
- [15] M. N. I. Jamaludin *et al.*, "An Effective Salp Swarm Based MPPT for Photovoltaic Systems Under Dynamic and Partial Shading Conditions," *IEEE Access*, vol. 9, pp. 34570–34589, 2021, doi: 10.1109/ACCESS.2021.3060431.
- [16] M. S. Bouakkaz, A. Boukadoum, O. Boudebouz, I. Attoui, N. Boutasseta, and A. Bouraiou, "Fuzzy Logic based Adaptive Step Hill Climbing MPPT Algorithm for PV Energy Generation Systems," in *2020 International Conference on Computing and Information Technology (ICCIT-1441)*, Tabuk, Saudi Arabia, 2020, pp. 1–5, doi: 10.1109/ICCIT-144147971.2020.9213737.
- [17] W. Hayder, A. Abid, M. B. Hamed, and L. Sbita, "Intelligent MPPT algorithm for PV system based on fuzzy logic," in *2020 17th International Multi-Conference on Systems, Signals & Devices (SSD)*, Monastir, Tunisia, 2020, pp. 239–243, doi: 10.1109/SSD49366.2020.9364195.
- [18] M. H. Salem, Y. Bensalem, and M. N. Abdelkrim, "MPPT based on P&O control and FLC-Hill Climbing technique for a Photovoltaic Generator," in *2021 18th International Multi-Conference on Systems, Signals & Devices (SSD)*, Monastir, Tunisia, 2021, pp. 589–594, doi: 10.1109/SSD52085.2021.9429453.
- [19] M. N. Ali, K. Mahmoud, M. Lehtonen, and M. M. F. Darwish, "An Efficient Fuzzy-Logic Based Variable-Step Incremental Conductance MPPT Method for Grid-Connected PV Systems," *IEEE Access*, vol. 9, pp. 26420–26430, 2021, doi: 10.1109/ACCESS.2021.3058052.
- [20] Bag, B. Subudhi and P. K. Ray, "A combined reinforcement learning and sliding mode control scheme for grid integration of a PV system," *CSEE Journal of Power and Energy Systems*, vol. 5, no. 4, pp. 498–506, Dec. 2019, doi: 10.17775/CSEEPES.2017.01000.
- [21] R. B. Roy *et al.*, "A Comparative Performance Analysis of ANN Algorithms for MPPT Energy Harvesting in Solar PV System," *IEEE Access*, vol. 9, pp. 102137–102152, 2021, doi: 10.1109/ACCESS.2021.3096864.
- [22] S. Padmanaban, C. Dhananjayulu, and B. Khan, "Artificial Neural Network and Newton Raphson (ANN-NR) Algorithm Based Selective Harmonic Elimination in Cascaded Multilevel Inverter for PV Applications," *IEEE Access*, vol. 9, pp. 75058–75070, 2021, doi: 10.1109/ACCESS.2021.3081460.
- [23] A. Raj and R. P. Praveen, "Highly efficient DC-DC boost converter implemented with improved MPPT algorithm for utility level photovoltaic applications," *Ain Shams Engineering Journal*, vol. 13, no. 3, pp. 1–9, 2022, doi: 10.1016/j.asej.2021.10.012.
- [24] R. Kahani, M. Jamil, and M. T. Iqbal, "An Improved Perturb and Observed Maximum Power Point Tracking Algorithm for Photovoltaic Power Systems," *Journal of Modern Power Systems and Clean Energy*, vol. 11, no. 4, pp. 1165–1175, 2022, doi: 10.35833/MPCE.2022.000245.
- [25] N. Kacimi, A. Idir, S. Grouni, and M. S. Boucherit, "An improved MPPT control strategy for PV connected to grid using IncCond-PSO-MPC approach," *CSEE Journal of Power and Energy Systems*, vol. 9, no. 3, pp. 1008–1020, 2022, doi: 10.17775/CSEEPES.2021.08810.
- [26] Ballaji, R. Dash, V. Subburaj, J. R. Kalvakurthi, D. Swain, and S. C. Swain, "Design & Development of MPPT Using PSO With Predefined Search Space Based on Fuzzy Fokker Planck Solution," *IEEE Access*, vol. 10, pp. 80764–80783, 2022, doi: 10.1109/ACCESS.2022.3195036.
- [27] Babes, F. Albalawi, N. Hamouda, S. Kahla, and S. S. M. Ghoneim, "Fractional-Fuzzy PID Control Approach of Photovoltaic-Wire Feeder System (PV-WFS): Simulation and HIL-Based Experimental Investigation," *IEEE Access*, vol. 9, pp. 159933–159954, 2021, doi: 10.1109/ACCESS.2021.3129608.
- [28] S. J. Zand, S. Mobayen, H. Z. Gul, H. Molashahi, M. Nasiri, and A. Fekih, "Optimized Fuzzy Controller Based on Cuckoo Optimization Algorithm for Maximum Power-Point Tracking of Photovoltaic Systems," *IEEE Access*, vol. 10, pp. 71699–71716, 2022, doi: 10.1109/ACCESS.2022.3184815.

- [29] A. Harrag and S. Messalti, "IC-based variable step size neuro-fuzzy MPPT improving PV system performances," *Energy Procedia*, vol. 157, pp. 362–374, 2019, doi: 10.1016/j.egypro.2018.11.201.
- [30] S. Padmanaban, N. Priyadarshi, M. S. Bhaskar, J. B. Holm-Nielsen, V. K. Ramachandaramurthy, and E. Hossain, "A Hybrid ANFIS-ABC Based MPPT Controller for PV System With Anti-Islanding Grid Protection: Experimental Realization," *IEEE Access*, vol. 7, pp. 103377-103389, 2019, doi: 10.1109/ACCESS.2019.2931547.
- [31] R. I. Areola, O. A. Aluko, and O. I. Dare-Adeniran, "Modelling of Adaptive Neuro-fuzzy Inference System (ANFIS)-Based Maximum Power Point Tracking (MPPT) Controller for a Solar Photovoltaic System," *Journal of Engineering Research and Reports*, vol. 25, no. 9, pp. 57–69, 2023, doi: 10.9734/jerr/2023/v25i9981.
- [32] D. Sarkar and P. K. Sadhu, "A novel fixed BIPV array for improving maximum power with low mismatch losses under partial shading," *IETE Journal of Research*, vol. 69, no. 11, pp. 8423–8443, 2023, doi: 10.1080/03772063.2022.2060871.
- [33] D. Sarkar and P. K. Sadhu, "GMPP Improvement with Fewer Power Peaks and Lower Mismatch Losses Using a New Hybrid BIPV Array Configuration," in *2023 5th International Conference on Energy, Power and Environment: Towards Flexible Green Energy Technologies (ICEPE)*, Shillong, India, 2023, pp. 1-6, doi: 10.1109/ICEPE57949.2023.10201617.
- [34] S. Bhattacharya, P. K. Sadhu, and D. Sarkar, "Performance evaluation of building integrated photovoltaic system arrays (SP, TT, QT, and TCT) to improve maximum power with low mismatch loss under partial shading," *Microsystem Technologies*, vol. 30, no. 5, pp. 583–597, 2024, doi: 10.1007/s00542-023-05564-0.

BIOGRAPHIES OF AUTHORS



Mohankumar Venugopal completed his doctoral degree under Visvesvaraya Technological University, Belagavi at Department of Electronics and Communication Engineering, Dr. Ambedkar Institute of Technology, Bangalore. His research interests are energy harvesting, control systems, and electronics and electrical circuits. He can be contacted at email: phd.mohankumar@gmail.com.



Madhusudhan Mahadevaswamy is a research scholar pursing his Doctoral degree under Visvesvaraya Technological University, Belagavi at electrical and electronics department, Dr. Ambedkar Institute of technology Bengaluru. His research interest is energy harvesting, high voltage engineering and electronics, and electrical circuits. He can be contacted at email: sudhanmadhu8111@gmail.com.



Manjunath Bimbitha Swarna Gowri is a research scholar pursing her Doctoral degree under Visvesvaraya Technological University, Belagavi at Department of Electronics and Communication Engineering, Dr. Ambedkar Institute of technology Bengaluru. Her research interest is energy harvesting and power electronics. She can be contacted at email: mbsgowri@gmail.com.